

SUPPORTING INFORMATION

Plasma-assisted nitrogen fixation in water with various metals

Pradeep Lamichhane<sup>a</sup>, Ramhari Paneru,<sup>a</sup> Linh N. Nguyen<sup>a</sup>, Jun Sup Lim<sup>a</sup>, Pradeep Bhartiya<sup>a</sup>, Bishwa Chandra Adhikari<sup>a</sup>, Sohail Mumtaz<sup>a</sup>, and Eun Ha Choi<sup>\*,a</sup>

1 Experimental setup

Photograph of the plasma jet and reaction cell utilized in this experiment is shown in Fig.S1. The plasma jet was created by embedding a 50.2 mm long stainless steel needle electrode with 0.9 mm external and 0.6 mm internal diameter inside a 72 mm long quartz tube of 4 mm external and 2 mm internal diameters. All joints was air sealed with the help of torr-seal. A 3 mm wide copper tape was utilized for ground electrode by folding over the quartz tube at 5mm underneath the tip of the needle. For the nitrogen-fixation in the liquid, a glass reaction cell covered by polystyrene lid was readied and the lower portion (10 mm) of the quartz tube was embedded through the cover as shown in Fig.S1. Dissimilar to the existing lightning and Birkeland–Eyde<sup>1</sup> nitrogen fixation procedure, background gas contamination was removed with the help of 2000 sccm  $N_2$  purging gas from the side hole of the cover. Based on the previous study,<sup>2,3</sup> nitrogen plasma in the same gas environment is the most favorable condition for ammonia synthesis.

when 1000 sccm  $N_2$  working gas was provided along with 10 kV (peak) and 33 kHz frequency from AC driven power source to the needle electrode, plasma was produced and engendered along the working gas stream. plasma plume directly interacts with the liquid surface which is at 3 mm below the nozzle of the quartz tube. To achieve the HER through the reduction of  $H^+$  ion, 5 gram of some common metals like Zinc (Zn), Aluminum (Al), Magnesium(Mg), Copper(Cu), were separately dipped in the 40 ml of deionized water electrolyte. The peripheral region of the reaction cell was also sealed by rubber washer and then the experiment was performed. and it's temperature was also always maintained at 18-20 °C with the help of temperature controlled system.

2 Methods and materials

2.1 Electrical characteristics

Current and voltage of the plasma discharged as measured using an oscilloscope (LeCroy wave surfer 434 MHz) with the current probe (LeCroy CP030) and high voltage (Tektronix P6015A).

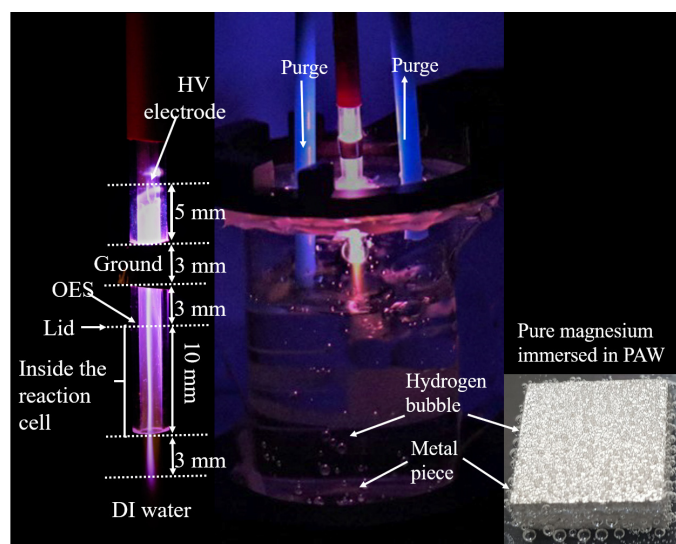


Fig.S1 Photograph of the atmospheric pressure non-thermal plasma source and reaction cell used for the nitrogen fixation process.

Discharge current ( $I$ ) from the acquired total current was evaluated from the deduction of background displacement current. The charge-voltage ( $Q$ - $V$ ) plot (Lissajous figures) of the current-voltage waveform shown in Fig.2 of the main text is presented in Fig.S2. The  $Q$ - $V$  plot becomes a closed-loop. It is a common technique to estimate the total energy dissipated in one cycle from the area of the  $Q$ - $V$  loop.<sup>4-6</sup>

The mean energy ( $p$ ) dissipation in this experiment was calculated as follows:<sup>7</sup>

$$p = \frac{1}{T} \int_{t=0}^{t=T} V(t)I(t)dt = f \times A_{\text{lissajous}} \quad (1)$$

Region within this Lissajous loop was determined as 215  $\mu J$ . All these presented experiment were carried out at  $p = E \times f = 7.1 W$

AC breakdown voltage for nitrogen gas at 1 cm electrodes gap in 1 atmospheric pressure is 22.8 kV, At the same condition discharge voltage for DC is 32 kV. Accumulation of wall charge on the dielectric surface in AC discharge is less than DC discharge. By owing to the fact that, breakdown voltage in AC discharge is

<sup>a</sup> Address, Department of Electrical and Biological Physics, Plasma Bioscience Research Center, Kwangwoon University, Seoul, Korea; Tel: +82-2-02-940-5662; \*E-mail: ehchoi@kw.ac.kr

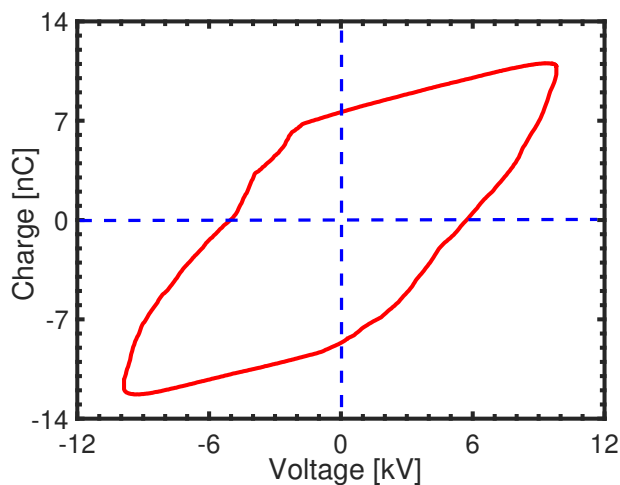


Fig.S2 The Lissajous figure of the plasma discharge [applied voltage: 10 kV, frequency: 33 kHz, working gas: nitrogen].

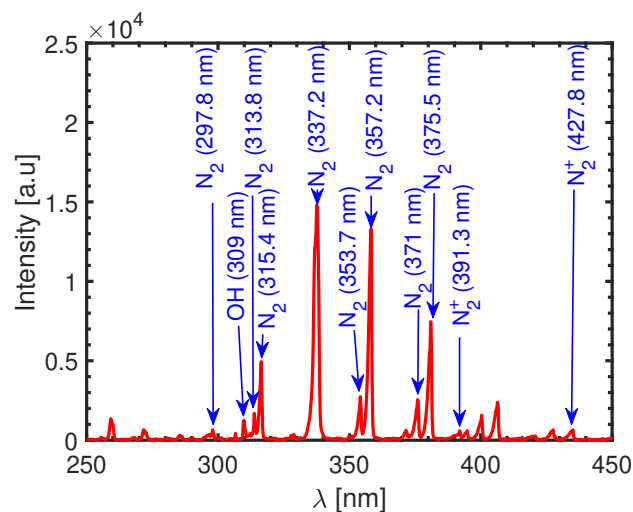
smaller as compared to DC discharge.<sup>8</sup> Thus, breakdown voltage and energy consumption rate in AC discharge is smaller as compared to DC discharge. We assumed that plasma-assisted  $\text{NH}_3$  synthesis could be a potential competitor of the H-B process in the future. But the energy consumption rate (=power/ $\text{NH}_3$  production rate) in plasma-assisted nitrogen fixation is in the range of few hundreds to thousand was  $\text{kWh/kg}$ , which is much higher than that of the H-B process (9–13  $\text{kWh/kg}$ ).<sup>3</sup> To reduce the energy consumption rate, discharge energy should be reduced (i.e. area of Lissajous loop should be small). Besides this, deposition of wall charges in DC discharge produce an opposite electric field which directly affects the production rate of reactive species after a long time plasma irradiation. Alternating charge flow cycle in AC discharge minimizes the accumulation of wall charges since the reactive species production rate in AC discharge is quite uniform as compared to DC discharge.

## 2.2 Optical characteristics

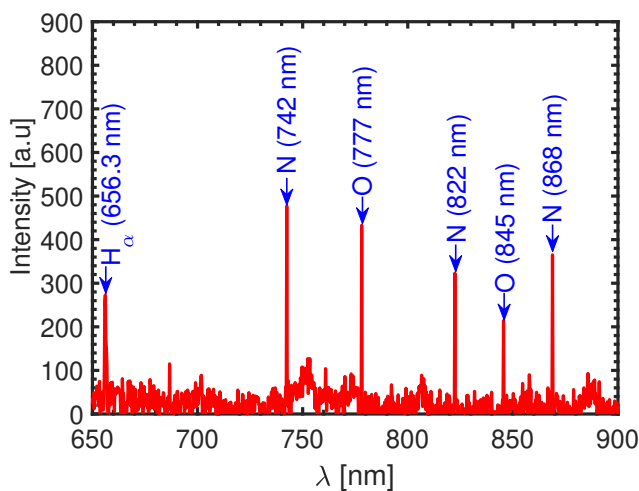
Optical emission spectroscopy (OES) of the nitrogen plasma was measured by the spectrometer (HR4000+CG-UV-NIR from Ocean Optics, Inc.) with the help of an optical fiber with a diameter of 400  $\mu\text{m}$  at a position of 3 mm downstream of the ground electrode. The spectrometer was calibrated for wavelength using an Hg-Ar lamp (Newport Corporation, model: 6048). OES within the range of 180 nm – 1100 nm is shown in Fig.4 of the main text whereas OES within the range of 250 nm- 450 nm and 650 nm-900 nm is further puffed and presented in Fig.S3(a) and S3(b), respectively.

## 2.3 $\text{NH}_3$ measurement

The  $\text{NH}_3$  concentrations were measured using an improved o-phthalaldehyde method<sup>9</sup> (QuantiFluo™ Ammonia Assay Kit from Bio-Assay Systems). In this method, solution with known  $\text{NH}_3$  concentrations [ 0  $\text{mgL}^{-1}$ , 4.25  $\text{mgL}^{-1}$ , 8.50  $\text{mgL}^{-1}$ , 17  $\text{mgL}^{-1}$ ] was prepared and 10  $\mu\text{L}$  aliquots was transferred to the



S3(a)



S3(b)

Fig.S3(a) OES within the range of 250 nm- 450 nm and Fig.S3(b) OES within the range of 650 nm- 900 nm [applied voltage: 10 kV, frequency: 33 kHz, working gas: nitrogen]

clear-bottom black 96 well-plate with 90  $\mu\text{L}$  detection reagent. Detection reagent was prepared by following the guidelines of the manufacturer. This reagent responds to  $\text{NH}_3$  within 15 minutes incubation in dark room and showed fluorescence at 450 nm when it was excited by 360 nm. The fluorescence intensity was recorded using a micro-plate reader (BioTeK Gen 5), which was relative to the  $\text{NH}_3$  concentrations.  $\text{NH}_3$  standard calibration curve is shown in Fig. S4. Similarly, fluorescence from the mixture of 10  $\mu\text{L}$  sample and 90  $\mu\text{L}$  detection reagent was also measured. By utilizing slope of standard calibration curve and fluorescence from the sample ( $F_{\text{sample}}$ ), we can estimate the concentration of  $\text{NH}_3$  in plasma activated water as follows:

$$[\text{NH}_3] = \frac{F_{\text{sample}} - F_{\text{blank}}}{\text{slope}} \times n \quad [\text{mgL}^{-1}]. \quad (2)$$

Where,  $F_{\text{blank}}$  is y-intercept of the standard curve [ fluorescence obtained from the detection reagent and pure water] and n is dilution factor. The  $\text{NH}_3$  concentration in our PAW is greater than

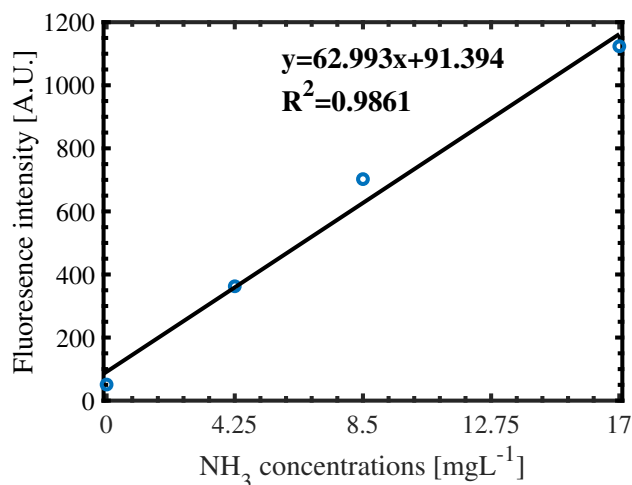


Fig.S4 Standard  $NH_3$  calibration curve obtained from known  $NH_3$  concentration versus 450 nm fluorescence plot. Fluorescence was obtained when detection reagent was excited by 360 nm.

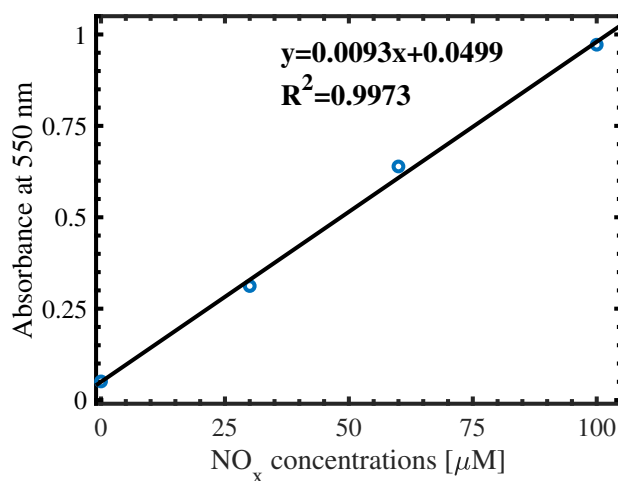


Fig.S5 Standard  $NO_x$  calibration curve obtained from known  $NO_x$  concentration versus 540 nm absorbance plot.

1mM (= 17 ppm = 17 mgL<sup>-1</sup>) so we diluted the PAW n times and to get the exact concentrations of  $NH_3$  we further multiply the result by the dilution factor n.

## 2.4 $NO_x$ measurement

Total concentration of dissolved  $NO$ ,  $NO_2$ , and  $NO_3$  [ $NO_x$ ] was measured using an improved Griess reagent kit<sup>10</sup> from Bio-assay system. It is a colorimetric method in which  $NO_x$  content in the sample was measured with the help of standard calibration curve obtained from the known concentration versus absorbance plot similar to the aforementioned  $NH_3$  measurement technique. Herein, we prepared a solution with known concentrations [0  $\mu M$ , 30  $\mu M$ , 60  $\mu M$ , 100  $\mu M$ ]. of these solution was mixed with 200  $\mu L$  of detection reagent prepared with the help of manufacturer's instructions. After the 60 minute incubation 250  $\mu l$  of these mixture from 300  $\mu l$  was transferred to the clear 96-well plate. This mixture gave absorbance at 540 nm which was measured by micro-plate reader. For the precise estimation of  $NO_x$  concentrations in the sample, absorbance versus concentration calibration curve was obtained which is shown in Fig.S5. To measure the  $NO_x$  concentration in the PAW, 100  $\mu l$  of PAW was mixed with detection reagent. After the incubation, absorbance given by mixture of PAW and detection reagent was measured ( $A_{sample}$ ). Actual concentration of  $NO_x$  in the sample was calculate as follows:

$$[NO_x] = \frac{A_{sample} - A_{blank}}{slope} \times n \quad [\mu M]. \quad (3)$$

Where,  $A_{blank}$  is y-intercept of the standard curve. Concentrations in our sample was higher than 100  $\mu M$  therefore sample was diluted and the concentration was obtained by multiplying the obtained results with dilution factor.

## 2.5 Temporal variations of $NO_x$ concentrations at various metal

The temporal variations in the  $NO_x$  concentrations of the PAW with Cu, Zn, Al during and after the plasma treatment are shown in the Fig.S6. The  $NO_x$  concentrations were almost similar to all metals immersed in the plasma-activated water.

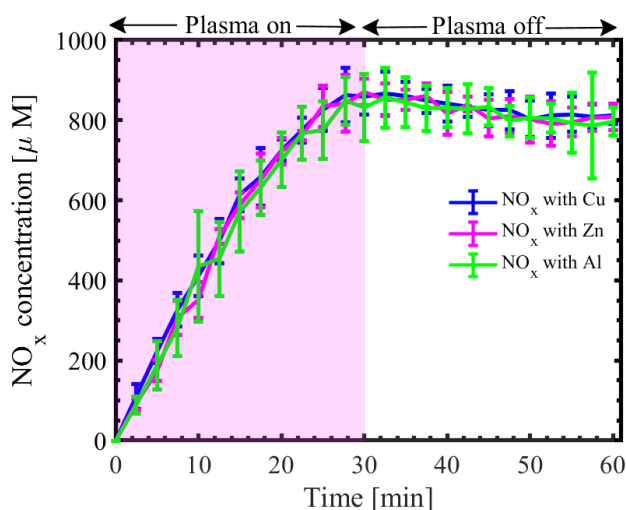


Fig.S6 Temporal variation of  $NO_x$  concentrations in the PAW for various metals during and after the plasma treatment

## 2.6 Hydrogen detection

Subsequent experiment was performed to verify the emission of nascent hydrogen from the reaction between plasma generated acid and metal. For this experiment, same volume of DI water was activated by plasma for 30 minutes. This PAW (pH  $\sim$  3.2) was transferred to another air sealed reaction cell with various metal similar with main experiment as shown in the Fig.S7. Evolved hydrogen gas ( $H + H \rightarrow H_2$ ) was detected from GasTech gas detection tube through the top hole of the lid for 3

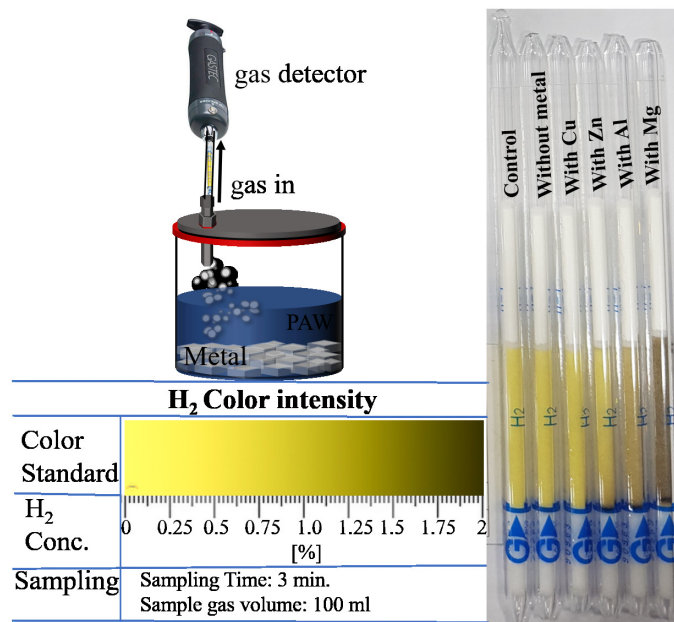


Fig.S7 Experimental setup for hydrogen detection and photograph of gas detection tube with color intensity

minute. When hydrogen gas enters into the gas detection tube, color of the detection tube is gradually converted into the yellowish brown and then blackish brown from yellow according to the H<sub>2</sub> concentration through the reaction  $H_2 + Na_2Pd(SO_3)_2 \rightarrow Pd + Na_2SO_3 + H_2SO_3$ . Concentration of hydrogen present in the 100 ml sample gas volume sucked by GasTech pump is measured with the help of color intensity bar given by the manufacturer.

## Notes and references

- 1 H. S. Eyde, *Journal of the Royal Society of Arts*, 1909, **57**, 568–576.
- 2 R. Hawtof, S. Ghosh, E. Guarr, C. Xu, R. M. Sankaran and J. N. Renner, *Sci. Adv.*, 2019, **5**, eaat5778.
- 3 P. Lamichhane, B. C. Adhikari, L. N. Nguyen, R. Paneru, B. Ghimire, S. Mumtaz, J. S. Lim, Y. J. Hong and E. H. Choi, *Plasma Sources Sci. Technol.*, 2020, **29**, 045026.
- 4 A. Gómez-Ramírez, J. Cotrino, R. Lambert and A. González-Elipé, *Plasma Sources Sci. Technol.*, 2015, **24**, 065011.
- 5 Y. Wang, M. Craven, X. Yu, J. Ding, P. Bryant, J. Huang and X. Tu, *ACS Catal.*, 2019, **9**, 10780–10793.
- 6 P. Lamichhane, B. Ghimire, S. Mumtaz, R. Paneru, S. H. Ki and E. H. Choi, *Journal of Physics D: Applied Physics*, 2019, **52**, 265206.
- 7 H. Jiang, T. Shao, C. Zhang, W. Li, P. Yan, X. Che and E. Schamiloglu, *IEEE Trans. Dielectr. Electr. Insul.*, 2013, **20**, 1101–1111.
- 8 C. Marshall, E. Matlis, T. Corke and S. Gogineni, *Measurement Science and Technology*, 2015, **26**, 085902.
- 9 S. S. Goyal, D. W. Rains and R. C. Huffaker, *Analytical Chemistry*, 1988, **60**, 175–179.
- 10 L. A. Ridnour, J. E. Sim, M. A. Hayward, D. A. Wink, S. M. Martin, G. R. Buettner and D. R. Spitz, *Anal. Biochem.*, 2000, **281**, 223–229.